

Growth of metal nanowires of tunable width

A. Klein, A. Schmidt, W. Meyer, L. Hammer, and K. Heinz

Lehrstuhl für Festkörperphysik, Universität Erlangen-Nürnberg, Staudtstr. 7, D-91058 Erlangen, Germany

(Received 7 December 2009; revised manuscript received 9 February 2010; published 18 March 2010)

Using scanning tunneling microscopy and low-energy electron diffraction it is demonstrated that the deposition of nickel on the hydrogen-stabilized (5×1) -H phase of Ir(100) leads to the formation of nickel nanowires of tunable widths and of lengths up to the order of $0.1 \mu\text{m}$. The tuning parameter is the number n of full monolayers deposited on the substrate: with that layer completed the next layer starts to grow by forming nanowires of n -atomic width whereby n is in the range $2 \leq n \leq 5$. The formation of the wires is interpreted as decoration or induction of stair rod dislocations which—as we reported earlier—develop to release the 9.0% pseudomorphic tensile strain of the full nickel layers. They lead to long sunk-in wedges at the surface whose width grows linearly with the number of layers deposited and so, by their decoration, nanowires of corresponding width develop. The wedges, and so the Ni wires, appear above single-atomic and macroscopically long Ir wires of the Ir(100)- (5×1) -H substrate which pin the dislocations. Above $n=6$, however, the films become rough and develop a squarelike patterning. It is speculated that the deposition of other metals with the same order of pseudomorphic strain should develop similar nanowires.

DOI: [10.1103/PhysRevB.81.115431](https://doi.org/10.1103/PhysRevB.81.115431)

PACS number(s): 61.46.-w, 68.35.-p, 68.47.De, 68.55.-a

I. INTRODUCTION

Nanostructures are an important issue in different kinds of scientific and technical fields. Due to expected new physical and chemical properties as well as the potential for special applications, they have attracted much interest in the recent past. So far, surface-lateral nanostructures are in most cases formed by self-assembly on especially structured surfaces in a bottom-up procedure, e.g., by the decoration of surface steps or special adsorption sites. To our knowledge only in a few cases it was possible to create nanowires of different widths on a single substrate, e.g., by the coverage-dependent decoration of the steps of a nearly (111) oriented platinum surface, so that wires of one- and two-atomic width develop.¹

In the present paper we demonstrate the preparation of nanowires which can be tuned to assume two-atomic up to five-atomic widths and lengths up to the order of $0.1 \mu\text{m}$. They are special in the sense that they need no surface steps to develop by decoration. The tuning parameter is the number of completed full nickel monolayers already deposited on a special substrate. The latter is the hydrogen-stabilized Ir(100)- (5×1) -H surface described in detail earlier²⁻⁵ and serves as an anisotropically nanostructured template. We shortly also describe the use of the clean Ir(100)- (5×1) -hex phase,^{6,7} which is also nanostructured but leads to nanowires of much lower quality, i.e., reduced lateral order and length. The investigations were performed using low-energy electron diffraction (LEED) and scanning tunneling microscopy (STM).

The paper is organized as follows. In the next section we recall in short the essentials of the structural properties of the two templates as determined earlier and provide details of the preparation of the nickel nanowires. Section III presents their characterization by STM and LEED. These results are discussed in Sec. IV, which is followed by the Conclusion.

II. PREPARATIONAL DETAILS

The preparation of the templates and nickel nanowires was performed within a stainless steel ultrahigh-vacuum

(UHV) chamber (2×10^{-11} mbar base pressure). The samples could be sputtered by noble gas ions as well as heated up to about 1500 K and cooled to about 90 K. A built-in electron-beam operated evaporator allowed for the deposition of nickel with a rate of about 0.3 ML/min (ML = monolayer) from a reservoir of 5 N purity. The templates and samples covered by full nickel monolayers were characterized by LEED intensity spectra for quality control through comparison with earlier investigations. This was realized using a three-grid LEED optics and application of a TV-based and computer-controlled intensity measuring procedure.⁸ From the preparation stage the samples could be transferred—without breaking the UHV—to a separate UHV chamber (operational pressure of $< 1 \times 10^{-11}$ mbar) provided with a STM (RHK beetle-type model UHV 300) allowing the investigation of the nanowires at room temperature. The STM was also used to determine the amount of nickel in the outermost layer (with the nickel layers below completed).

The two templates Ir(100)- (5×1) -hex and Ir(100)- (5×1) -H were prepared as described in earlier work.^{2,7} We recall that Ir(100)- (5×1) -hex is characterized by a quasi-hexagonally close-packed surface layer, which—as it resides on quadratic layers below—is considerably buckled. In contrast, in the Ir(100)- (5×1) -H phase the hexagonal reconstruction is lifted by hydrogen, so that the extra atoms of the former hexagonal layer are expelled to a new surface layer where they arrange as long wires of atomic width. Their spacings are dominantly $5a_{Ir}$ [with $a_{Ir}=2.715 \text{ \AA}$, the in-plane lattice parameter of Ir(100)]. This is also the average spacing as occasionally occurring values of $3a_{Ir}$ are followed by a $7a_{Ir}$ spacing (or vice versa).

III. NANOWIRES WITH TUNABLE WIDTH

In the following the emphasis is on the nanowire formation on the (5×1) -H phase (Sec. III A). That on the (5×1) -hex phase is addressed only shortly as the local struc-

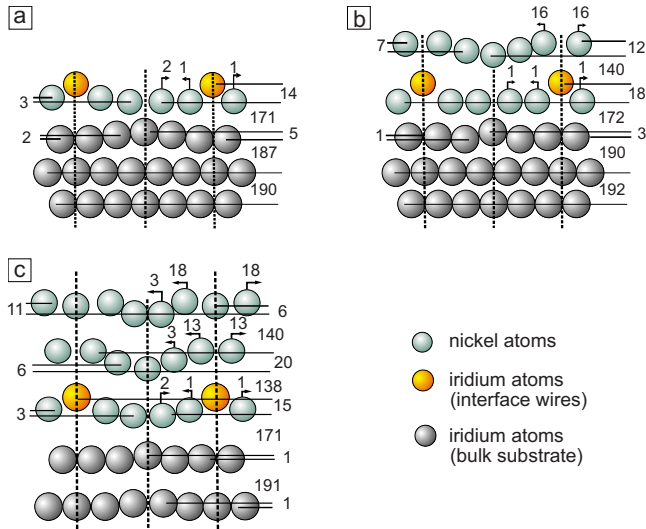


FIG. 1. (Color online) Structural models for (a) 0.8, (b) 1.8, and (c) 2.8 ML Ni deposited as resulting from LEED analyses (Refs. 10–12). The structural parameters given are in pm units. Note that neighbored layers are displaced with respect to each other by half a lattice parameter perpendicular to the drawing plane and vertical spacings and bucklings are exaggerated for better visibility of the structure.

ture is the same but the order and length of the wires are much poorer (Sec. III B).

A. Nanowires on Ir(100)-(5×1)-H

The deposition of nickel or other transition metals such as iron or cobalt on the (5×1)-H phase at room temperature leads, as reported earlier,^{9,10} to the filling of the space between the iridium wires (equivalent to a coverage of 0.8 ML). The corresponding structural ball model is displayed in Fig. 1(a). The next now full Ni monolayer ($n=1$, i.e., 1.8 ML total coverage) resides carpetlike on the mixed Ni₄Ir interface layer as displayed in Fig. 1(b). The ball model for the second full monolayer deposited ($n=2$) is displayed in Fig. 1(c) (all ball models result from quantitative LEED).^{10–12} Neglecting the slight buckling of the full layers all films suffer from a 9.0% tensile strain due to the different in-plane lattice parameters of Ir and Ni ($a_{Ir}=2.715$ Å, $a_{Ni}=2.490$ Å).

The deposition of a few percent of a monolayer on the $n=2$ film leads to the appearance of long wires as displayed in Fig. 2(a). Zooming nearer to a single wire reveals that it is of two-atomic width as apparent from Fig. 2(b) and in more detail in Fig. 2(d). It is also evident from the height profile given in Fig. 2(c), which runs along the line inserted in Fig. 2(b). The length of these wires is on the order of the Ir wires at the interface and they are positioned right above the latter as it results from the comparison of the morphologies of the bare substrate and the films together with quantitative LEED structure determination. Continuing Ni deposition makes the wires coalesce until another full metal layer is completed ($n=3$). The next layer growth again starts by forming long nickel wires [Fig. 2(e)], yet now of three-atomic width [Figs. 2(f)–2(h)].

This growth type proceeds whereby wires of four-atomic width on the $n=4$ film [Figs. 2(i)–2(l)] and of five-atomic width on the $n=5$ film [Figs. 2(m)–2(p)] form. However, laterally separated wires become increasingly rare and are frequently attached to each other. Additionally we observe that the growth mode changes significantly at $n>5$ as demonstrated in Fig. 3. The wires—which continue to form—become increasingly cross linked eventually leading to a rough and squarelike nanopatterned film.

B. Nanowires on Ir(100)-(5×1)-hex

As mentioned in the Introduction the clean and stable (100) surface of iridium, Ir(100)-(5×1)-hex, can also be used as a nanostructured template. As described in detail previously, its quasi-hexagonally close-packed top layer arranged on the square layers below forms troughs of 0.5 Å depth.⁷ These in fact act as preferred adsorption channels for metals such as Fe, Co, and Ni.^{12,13}

However, as shown in detail earlier,¹³ the hexagonal reconstruction is lifted already at submonolayer coverage. Obviously, the extra atoms accommodated in the hexagonal layer and expelled to the very surface form only short chains with little lateral order between which the Ni atoms accommodate. So, the modulation of a film is of low order as demonstrated in Fig. 4(a) for a $n=3$ film. As a consequence, the developing nickel nanowires are of reduced length and equally poor order and frequently appear to have coalesced as displayed in Fig. 4(b).

IV. DISCUSSION

We have demonstrated that by Ni deposition on Ir(100)-(5×1)-H nanowires of well-defined width develop. In atomic diameter units it equals the number n of full monolayers already deposited (not counting the mixed interface layer), i.e., nickel wires of n -atomic width form on the n th full monolayer. This is for $n=2–5$, i.e., the development of separated wires stops at $n=5$ above which the film growth becomes three dimensional and the films become increasingly nanopatterned in a squarelike way.

For the interpretation of our findings we recall recent results we have obtained for Ni growth on the unreconstructed surface of iridium, Ir(100)-(1×1), by using LEED and STM as well as calculations applying density-functional theory (DFT).¹¹ We observed narrow and sunk-in wedges in completed layers for $n=3–5$. Consistently, DFT calculations revealed that flat Ni layers pseudomorphic with Ir(100)-(1×1) are unstable for $n\geq 3$ and that the tensile stress buildup in the films is (at least partly) released by the formation of stair-rod-like dislocations. This was also confirmed by independent stress measurements.¹⁴ We additionally found that on Ir(100)-(5×1)-H the wedges develop right above the Ir wires at the interface. So they exhibit their regular arrangement allowing to be accessed by quantitative LEED (Ref. 11) revealing that they are sunk in by about 0.2 Å in agreement with the apparent height retrieved by STM.

Figure 5(a) displays the structure obtained for $n=3$. We have changed the shading of top layer nickel atoms not be-

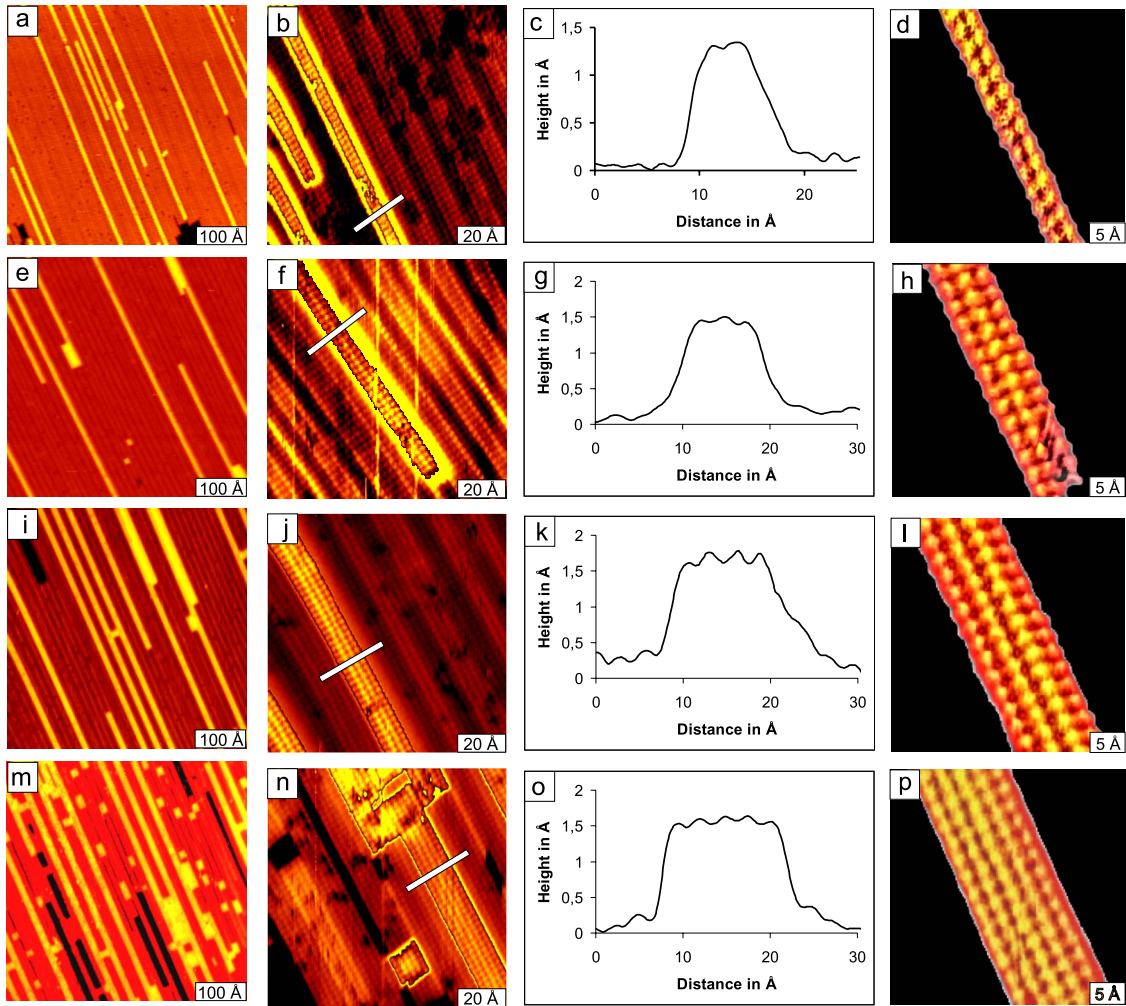


FIG. 2. (Color online) Nickel nanowires of two- to five-atomic width (panels in subsequent rows) prepared on Ir(100)-(5×)-H. The STM images in the first column panels are on a large scale, those in the second exhibit already atomic resolution which is much improved in the fourth column panels (the tip voltages and tunnel currents used are in the ranges 1–3 mV and 3–8 nA, respectively). The height profiles displayed in the third column panels are along the lines inserted in the images of the second column.

longing to the wedge to visualize our interpretation of the development of wires of two-atomic width on the completed $n=2$ nickel film: we propose that the appearance of the dis-

location does not need a fully completed $n=3$ layer but is induced locally already when this layer starts to grow. Atoms arriving on the completed $n=2$ layer dig their energetically most favorable sites vertically above the interface iridium wires by inducing the wedge in a ziplike way. Indeed, inspection of the local atomic positions of the additional Ni atoms completing the third layer [light shaded atoms in Fig. 5(a)] indicates that they lack strong interactions with the

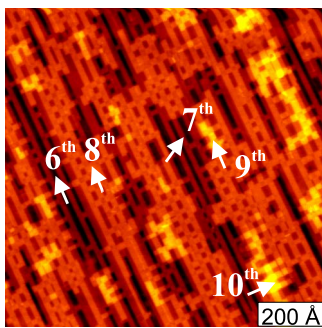


FIG. 3. (Color online) STM image of a Ni film on Ir(100)-(5×1)-H at a total coverage of about $N=7$ ML ($U_{tip}=-0.46$ V, $I=4.2$ nA). Layer N and layers below are not yet fully completed and Ni atoms appear already in layers above the N th one.

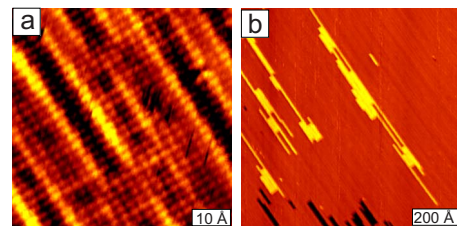


FIG. 4. (Color online) STM images for nickel films on the Ir(100)-(5×1)-hex substrate for (a) an atomically resolved $n=3$ film ($U_{tip}=-102$ mV, $I=9.21$ nA) and (b) the same film on a larger scale ($U_{tip}=-9.42$ mV, $I=2.96$ nA).

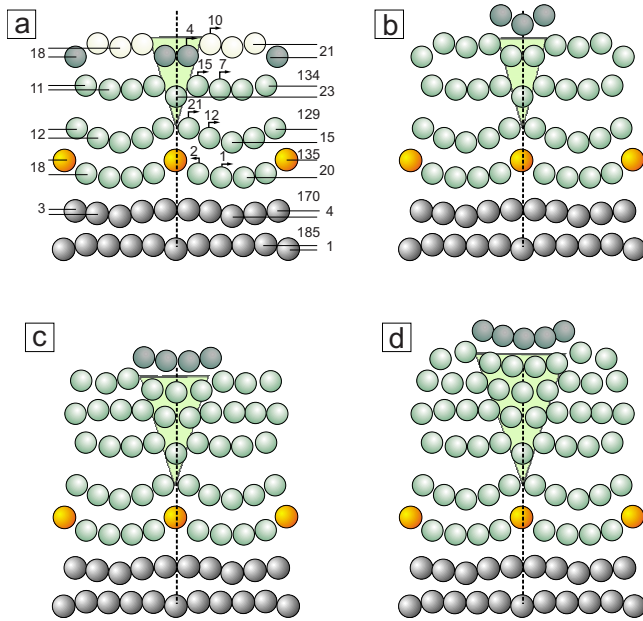


FIG. 5. (Color online) Ball models for the structure of nickel wires of two- to five-atomic width [(a)–(d), respectively]. In (a) the structural parameters (in pm units) are given as resulting from a structure determination by quantitative LEED (Refs. 11 and 12). The vertical scaling is the same as in Fig. 1.

wedge and just decorate the already existing structure. On the other hand, with the layer completed ($n=3$) there are already sunk-in wedges which for additionally arriving atoms offer energetically preferred fourfold sites, so that wires of three-atomic width develop [Fig. 5(b)]. This procedure repeats for the next two layers ($n=4,5$) so that with the wedge becoming broader wires of four- and five-atomic width grow [Figs. 5(c) and 5(d)].

As observed, the wires are not always laterally separated for $n=4$. Also, $n=5$ wires appear more rarely than wires of smaller width. With the dominant spacing between the interface Ir wires (and so between the centers of the wedges) being $5a_{Ir}$ and as an occasional $7a_{Ir}$ spacing must be followed by a $3a_{Ir}$ spacing, $n=5$ nickel wires correspond to the maximum width. When such wires form above neighbored Ir chains they just touch each other, i.e., they are no more isolated. Additionally, we observe a change in the growth mode for $n > 5$ with the surface becoming rough and nanopatterned in a squarelike way with increasing coverage (Fig. 3). This is probably due to the fact that the formation of stair rod dislocations in the range $n \leq 5$ reduces only unidirectional stress vertical to the wires, while the films remain by 9.0% strained in the direction orthogonal to that. Although there is no detailed model at hand we regard the cross linking of nanowires by the connection of wires of the same width and the development of square patterned films with increasing coverage as the films' reaction to release stress and strain in the two intrasurface directions. Independent stress measurements have indeed shown that two different stress release scenarios exist.¹⁴

Basically the same growth procedure of nickel wires holds also for the clean and hexagonally reconstructed iridium template, Ir(100)-(5 × 1)-hex. The reconstruction is

lifted already by some fraction of a nickel monolayer deposited. Similar to restructuring induced by hydrogen the Ir atoms additionally accommodated in the hexagonal layer are expelled to the surface, however, in a rather different way. The hydrogen-induced process starts at surface defects as there the energy cost to expel the additional Ir atoms is reduced. Once this is started hydrogen induces that further atoms of the hexagonal layer are expelled in a zipper way, so that long linear atomic iridium chains form in a new layer.^{2,3} The dominant spacing of the chains is $5a_{Ir}$, as only the 20% extra atoms accommodated in the hexagonal layer can be expelled. In contrast, the lifting of the reconstruction by nickel atoms is induced locally where nickel atoms happen to arrive on the surface. So, only short iridium chains are formed, more or less statistically distributed on the surface, i.e., with rather poor lateral order. As a consequence, the lateral order of the nickel wires developing on this surface is evenly poor, i.e., poorer than that observed on Ir(100)-(5 × 1)-H.

This fact eventually leads to the question concerning the role of hydrogen with respect to the growth of the nickel wires. We know that on the (5 × 1)-H phase the hydrogen atoms reside on the very surface occupying bridge sites both on the iridium chains and on the (1 × 1) terraces between them.⁵ Upon initial deposition of nickel the hydrogen atoms on the terraces desorb, while those on the iridium chains remain there, even for increasing nickel coverage.¹⁰ They seem to have little influence on the structure as the LEED intensity spectra recorded for nickel films prepared on the (5 × 1)-H and (5 × 1)-hex phases are very similar¹⁰ and so locally the underlying structure must be very similar, too.

V. CONCLUSION

In conclusion we have found that nickel nanowires of n -atomic width for $n=2-5$ can be formed in a controlled way on the Ir(100)-(5 × 1)-H template. These wires reside on a nickel film consisting of n pure nickel layers and a Ni₄Ir interface. The adsorption channels allowing for the formation of the wires come by stress-releasing formation of wedgelike stair rod dislocations which preferably develop above the iridium wires at the interface. For the two-atomic wires these wedges are induced by the nickel atoms arriving on the completed layer $n=2$. For $n=3-5$ they grow by decoration of the wedges already present which offer preferred adsorption channels increasing in width linearly with n . Of course, similar nanowires should grow also for other materials provided they suffer from a similar magnitude of pseudomorphic tensile stress as nickel. It should be also possible to create nanowires of another atomic species than that of the film on which they reside. One might speculate that possibly (magnetic) nickel nanowires on a nonmagnetic film can be grown, so that isolated nanomagnets could be formed. A candidate to use for the film might be copper which would exhibit also a considerable tensile strain ($\approx 6.5\%$) when growing on Ir(100).

ACKNOWLEDGMENT

The authors are indebted to Deutsche Forschungsgemeinschaft (DFG) for financial support.

- ¹P. Gambardella, M. Blanc, K. Kuhnke, K. Kern, F. Picaud, C. Ramseyer, C. Girardet, C. Barreateau, D. Spanjaard, and M. C. Desjonquères, *Phys. Rev. B* **64**, 045404 (2001).
- ²L. Hammer, W. Meier, A. Klein, P. Landfried, A. Schmidt, and K. Heinz, *Phys. Rev. Lett.* **91**, 156101 (2003).
- ³K. Heinz and L. Hammer, *Z. Phys. Chem.* **218**, 997 (2004).
- ⁴K. Heinz and L. Hammer, *J. Phys. Chem. B* **108**, 14579 (2004).
- ⁵D. Lerch, O. Wieckhorst, L. Hammer, K. Heinz, and S. Müller, *Phys. Rev. B* **78**, 121405(R) (2008).
- ⁶A. Ignatiev, A. Jones, and T. Rhodin, *Surf. Sci.* **30**, 573 (1972).
- ⁷A. Schmidt, W. Meier, L. Hammer, and K. Heinz, *J. Phys.: Condens. Matter* **14**, 12353 (2002).
- ⁸K. Heinz, *Rep. Prog. Phys.* **58**, 637 (1995).
- ⁹K. Heinz, L. Hammer, A. Klein, and A. Schmidt, *Appl. Surf. Sci.* **237**, 519 (2004).
- ¹⁰C. Giovanardi, A. Klein, A. Schmidt, L. Hammer, and K. Heinz, *Phys. Rev. B* **78**, 205416 (2008).
- ¹¹A. Klein, W. Meyer, A. Schmidt, B. Gumler, S. Müller, L. Hammer, and K. Heinz, *Phys. Rev. B* **78**, 045422 (2008).
- ¹²K. Heinz and L. Hammer, *Prog. Surf. Sci.* **84**, 2 (2009).
- ¹³L. Hammer, W. Meier, A. Schmidt, and K. Heinz, *Phys. Rev. B* **67**, 125422 (2003).
- ¹⁴Z. Tian, C. S. Tian, D. Sander, and J. Kirschner, *Verhandl. DPG* **41**, 465 (2006).